DOI 10.5162/EUROSENSORS2025/MP55

C-V measurement of Schottky Barrier LSMO/Nb:STO heterostructure dedicated to optoelectronic devices

Fallou Gning[1], *Jeremy Blond*[1], *Victor Pierron*[1], *Laurence Méchin*[1], *Bruno Guillet*[1]
[1] *Caen Normandy University, ENSICAEN, CNRS, Normandy Univ., GREYC, UMR6072, F-14000 Caen, France*
fallou.gning@unicaen.fr, bruno.guillet@unicaen.fr

Summary:

This study investigates the electrical properties of the Schottky diode based on the heterostructure formed by the association of a $La_{2/3}Sr_{1/3}MnO_3$ (LSMO) thin film with a 0.01 %wt Nb-doped $SrTiO_3$ (Nb:STO) substrate. Capacitance-voltage (C–V) measurements in reverse bias were carried out at 100 kHz from 300 K to 380 K. The dopant concentration of substrate and the Schottky Barrier Height were extracted from the $1/C^2$–V curve fit. The results show a systematic increase in both parameters with temperature, affecting the space-charge region and shifting the spectral response from near-infrared to visible. These results highlight the importance of a good knowledge of oxide interface electrical properties and also the potential of oxide thickness engineering for improving diode photodetection efficiency.

Keywords : Oxide heterostructure, Schottky diode, C-V characteristics, Nb:STO, LSMO

Motivation

Oxide-based heterostructures have emerged as a promising platform to explore novel electronic phenomena at interfaces due to their distinctive electrical properties and multifunctional potential [1]. In particular, the nobium-doped $SrTiO_3$ (Nb:STO), with a bandgap of 3.25 eV [2], is a suitable candidate for ultraviolet (UV) photodetection, while the Schottky Barrier Height (SBH) Φ_{Bf} of approximately 0.92 eV at the LSMO/Nb:STO interface [3] is appropriate for visible and near-infrared sensing. This work aims to provide a detailed understanding of the junction characteristics by extracting the doping level and SBH from C–V measurement under various temperatures. This constitutes the baseline for a future design of an optoelectronic sensing device.

Heterostructure Fabrication

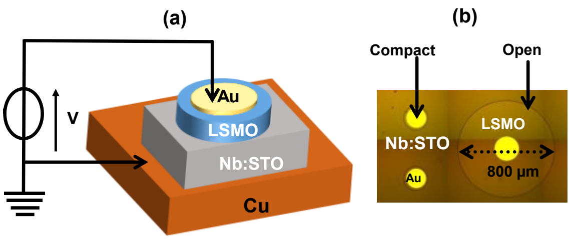

Figure 1 : (a) Cross-section diagram of the LSMO/Nb:STO heterojunction b) Examples of different heterojunction geometries

The studied samples were fabricated on lightly-doped single-crystal STO substrates at 0.01 wt% Nb content with two different thin LSMO films 10 nm and 20 nm epitaxially grown using Pulsed Laser Deposition (PLD) at 730°C. A 130 nm gold top electrode (Au) was also deposited at room temperature by Ion Beam Deposition (IBD), defining the contact on LSMO anode. The cathode was contacted using a copper plate (Cu) bonded to the back of the substrate with silver-paste. Circular heterostructures compact and open as on Figure 1 were defined on each sample by UV photolithography and chemical/ion etching. The open was used just to identify the effective surface area, enabling measurements to be normalized.

Results

C–V characteristics were measured under dark conditions using a Keithley 590 CV analyzer at 100 kHz over the temperature range of 300 K to 380 K, in steps of 20 K on the compact LSMO/Nb:STO heterojunction for each sample.

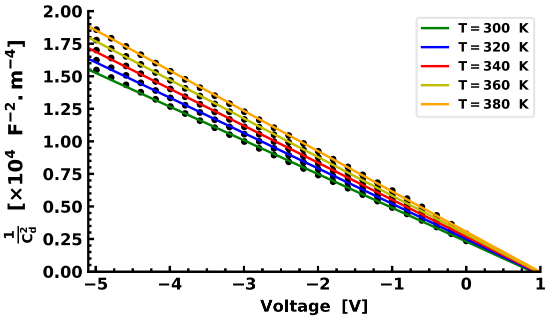

Figure 2 : Evolution of $1/C^2$ with voltage of the compact LSMO/Nb:STO heterojunction for 20 nm thick

As shown in Figure 2, linear 1/C²-V characteristics between -5 V and 0 V were revealed. This behavior is consistent with the independence of the relative permittivity ε_r of lightly doped Nb:STO from the electric field [4]. The latter decreases between 300 K and 400 K, according to Figure 3 plotted using Barrett's formula [5] where b(T) was assumed to be linearly dependent upon temperature. In this case, the N_d doping concentration and Φ_{Bf} will be extracted by linear fitting using eq.(1) [5]. As illustrated in Figures 4a and 4b, an increase in Schottky Barrier Height and doping concentration as a function of temperature was observed. The Nb doping concentrations are of the same order as the theoretical value of 3.1×10^{18} cm^{-3} expected for 0.01 wt% doped Nb:STO substrates. This evolution has an impact on the expected width of the Space Charge Region (SCR) eq.(2) [5] (see Figure 5), which broadens with reverse bias and constricts with temperature (relative permittivity decrease). These variations impact the spectral response of the devices, as the SBH value is determining the absorption cut-off wavelength of the Schottky diode for the internal photoemission process [6]. Higher barriers 1.21–1.36 eV for the 10 nm thick LSMO anode shorten the cut-off slightly wavelength to 0.91–1.02 µm, while lower barriers 0.89–0.99 eV for the 20 nm thick anode extend the cut-off wavelength 1.25–1.40 µm in the Near-InfraRed (NIR) band. This demonstrates ability to target specific spectral regions by adjusting only LSMO thickness.

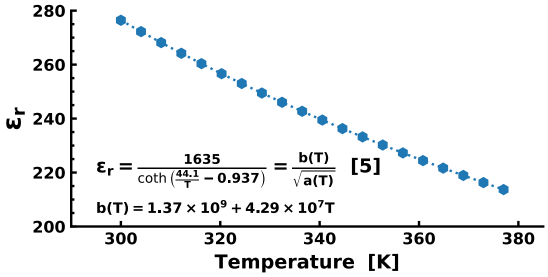

Figure 3 : Variation of relative permittivity for 0.01%wt doped Nb:STO with temperature, with zero electric field

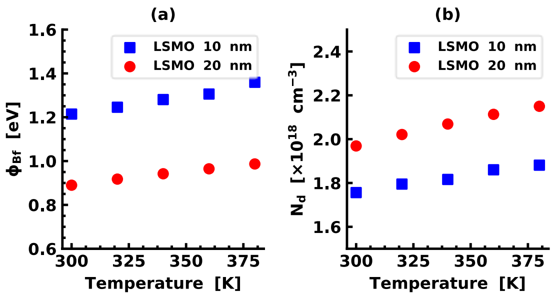

Figure 4 : Temperature dependence of (a) Schottky Barrier Height and (b) doping concentration N_d.

$$\frac{1}{C_d^2} = \underbrace{\frac{2\sqrt{a(T)}}{b(T)\varepsilon_0 q N_d}\phi_{Bf}}_{\alpha} - \underbrace{\frac{2\sqrt{a(T)}}{b(T)\varepsilon_0 q N_d}}_{\beta} V = \alpha + \beta V \qquad (1)$$

$$W_{SCR_{max}} = \frac{b(T)\varepsilon_0}{qN_d} cosh^{-1}\left[1 + \frac{qN_d}{\sqrt{a(T)}\,b(T)\varepsilon_0}\left(\phi_{Bf} - V\right)\right] (2)$$

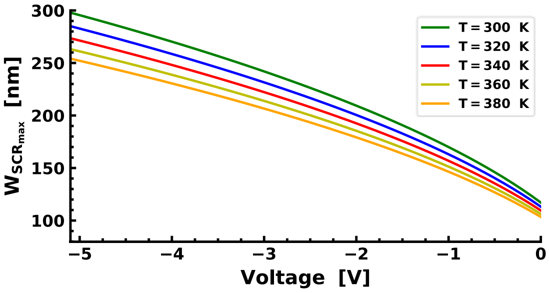

Figure 5 : Evolution of the expected Space Charge Region width versus applied reverse voltage of the compact LSMO/Nb:STO heterojunction for 20 nm thick

Conclusion

The results of this study highlight the sensitivity of oxide junctions to temperature and design parameters, which is crucial for developing performant optoelectronics devices. The observed modification of the Schottky Barrier Height versus the LSMO thickness could be interesting in developing wavelength-selective optoelectronic oxide devices. A study taking into account the frequency-dependent behavior of this to better understand the interface physics and transport mechanisms in such LSMO/Nb:STO heterostructure will be part of a future work.

References

[1] C. A. F. Vaz et al. *J. Phys. Condens. Matter* 27 123001 (2015); doi: 10.1088/0953-8984/27/12/123001

[2] S. Ramanathan, Thin Film Metal-Oxides, Chap. 5 (2010); doi: 10.1007/978-1-4419-0664-9

[3] K. G. Rana, et al., Phys. Rev. B 87 (2013); doi: 10.1103/PhysRevB.87.085116

[4] S. Suzuki et al., J. App. Phys., 81, 6830 (1997); doi: 10.1063/1.365242

[5] T. Yamamoto et al., J. App. Phys., 37, 4737 (1998); doi: 10.1143/JJAP.37.4737

[6] S. M. Sze, *Physics of Semiconductor Devices*, Ed. 3 (2007); doi: 10.1002/0470068329